

## 4. Analysis of NOMA: In Capacity Domain

Saurabh Srivastava, Dept. of EC, BIT, Mesra, Ranchi, India [saurabhnitkian@gmail.com](mailto:saurabhnitkian@gmail.com)  
Prajna Parimita Dash, Dept. of EC, BIT, Mesra, Ranchi, India [ppdash@bitmesra.ac.in](mailto:ppdash@bitmesra.ac.in)  
Sanjay Kumar, Dept. of EC, BIT, Mesra, Ranchi, India [skumar@bitmesra.ac.in](mailto:skumar@bitmesra.ac.in)

### ABSTRACT

*Non-orthogonal multiple access (NOMA) is supposed to be used for forthcoming 5G cellular networks. In this paper, the expressions for the channel capacities for symmetric and asymmetric NOMA networks have been analyzed. The performance measure of user spectral efficiency and the sum-rate bounds, for the NOMA and the existing OMA networks have been compared. Furthermore, analysis of user rate and capacity of NOMA network has been carried out and observed that the NOMA capacity region varies as a function of the power allocation factor. The corresponding models have been developed for both uplink and downlink, and simulated with MATLAB. The experimental results show that even in the symmetric channel conditions, NOMA is able to perform and provides the same spectral efficiency as OMA.*

**Keywords**—OMA, NOMA, rate-region, spectral efficiency, power allocation factor

### INTRODUCTION

The mobile communication has come through various generations over a little span of time. The motivating factor for every next generation is marked with higher user data rate and enhanced user service. Though the current 4G cellular standard provides a high data rate, the requirement of high data rate is massively increasing. Moreover, the variety of user services such as massive machine type communication (mMTC), ultra-reliable low latency communication (URLLC) and enhanced Mobile Broadband (eMBB) demand new architectures and configurations for the upcoming 5G cellular services.

It is also expected that the number of connected devices to reach 29 billion by 2022 [1], out of which 1.5 billion would be Internet of Things (IoT) devices. These massive connections characterize high connection volumes as well as small data traffic volumes and on the other contrary, they require ultra-reliability, availability, low latency high throughput etc. The current 4G cellular is not able to fulfil these diverse requirements, as the 4G vision is centred on cellular mobile and not focused on these diversified cases. Thus, 5G has to come up with the solutions to the above cases. The next generation mobile networks (NGMN) alliance provides the vision for 5G, while discussing these cases [2]. Specifically, it mentions the improvements required in spectral efficiency of the cell (bps/Hz/cell) and user spectral efficiency (bps/Hz/user) for supporting the massive connectivity between users as well as devices.

The major objective in the cellular generations has been to achieve a larger user capacity, and return a larger sum-capacity. A large sum-rate signifies an efficient network by maximizing each user's throughput to its capacity. So, the objective across the generations has been to maximize the sum-rate. Moreover, the 5G network is also supposed to cater a number of other key performance indicators such as a reduced latency (user-plane) of about 1 ms for eMBB and URLLC applications; and energy efficiency in eMBB use case [3]. The above performance indicators suggest a new waveform design or specifically a multiple access scheme that provides a higher spectral efficiency, high energy efficiency, lower latency, more user-fairness and massive connectivity for device to device communication and IoT.

Since the waveform design has been the most fundamental aspect of the physical layer, the signalling and multiple access formats have significantly changed over the cellular generations. The analog Frequency Modulation (FM) and Frequency Division Multiple Access (FDMA) based 1G systems got transformed into a digital Time Division Multiple Access (TDMA)/FDMA based 2G systems. The focus of all the global 3G systems was on Code Division Multiple Access (CDMA). Further, due to increasing bandwidth requirements Orthogonal Frequency Division Multiple Access (OFDM) that was adopted in 4G, as (Orthogonal Frequency Division Multiple Access (OFDMA). OFDM offered several advantages compared to its predecessors, like

computationally efficient implementation and simple equalization [4]. The foremost flaws of OFDM include its high peak-to-average-power ratio (PAPR), and the requirement of strict orthogonality among its subcarriers.

All the existing multiple access techniques have been utilizing the orthogonality between their shares in the resource block. For TDMA, the resource block is time, and different users are allowed to communicate only in their respective time slot. In FDMA and OFDMA, the users are differentiated in frequency domain and permitted communication only during their frequency slots. In CDMA, although the users can use entire time/frequency resource block, but are differentiated with orthogonal spreading codes.

Hence, these can be classified as orthogonal multiple access (OMA) schemes. The major concern of the provision of massive connection density and high capacity for eMBB and low latency for URLLC communication the 5G networks specify the current spectrum utilization to be made more efficient. One of the mechanism is simply allocating more users within a resource block, avoiding the orthogonality restriction between the users. In this regard, Non-Orthogonal Multiple Access (NOMA) is treated as the best candidate for 5G cellular networks [5]. NOMA simply allocates more than one user to a resource block. Currently, with 4G OFDMA, each resource block is allocated to a single user. Hence, a significant increase in capacity can be observed theoretically, if each resource block is shared among several users, and each user completely utilizes the whole resource block. Thus, NOMA provides system overloading [6], which is highly desirable for massive connection density. In NOMA, the user's utilize the complete resource block and transmit simultaneously without being differentiated in time/ frequency/code domain. The receiver differentiates the users either based on the different user power levels or by different sparse (spreading) codes that are non-orthogonal.

In this paper, we evaluate the effect of power allocation factor on the capacity region of NOMA in the downlink as well as in the uplink scenarios. For the downlink case, we assume a single transmitting antenna at the BS and two different user devices as receivers. The uplink scenario consists of the user devices transmitting to the BS antenna. In the downlink, the superposition coding (SC) is performed by the BS, and successive interference cancellation (SIC) is done by the user equipment (UE). On the contrary, SIC is done at the BS in the uplink.

The rest part of the paper is organized as follows. Section II presents the related work with NOMA classification. This section highlights the characteristics of Power Domain (PD) NOMA, and the processes involved at the transmitting and receiving ends of the system. Section III identifies the performance metrics of the proposed system, specifically defining the capacity, spectral efficiency, user-rates and the sum-rate.

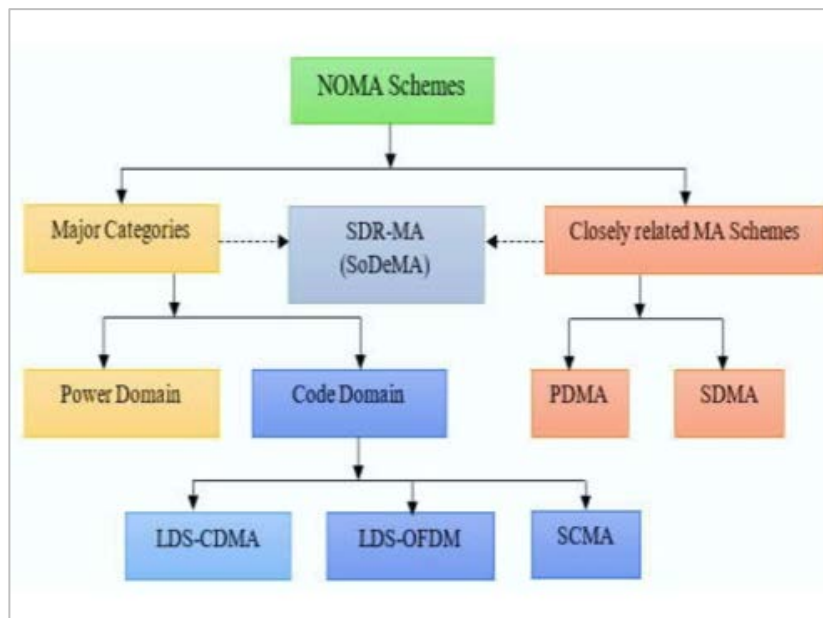


Figure 4-1 Classification of NOMA and similar schemes

In section IV, we describe the proposed system model for carrying out the analysis of the capacity region in PD-NOMA network. In this section, we evaluate the rate-region depending upon the received signal-to-noise+interference ratio (SINR). We also deal with the mathematical analysis of the symmetric and asymmetric cases and thus obtain the rate-region variation based upon the SINR. As far as our knowledge is concerned, no such in-depth analysis has been presented in the available literatures that takes both of the cases into account. Section V describes the simulation parameters and interprets the results obtained with MATLAB. Finally, section VI concludes the paper justifying the candidature of NOMA as a future multiple access scheme.

## RELATED WORK

NOMA refers to a new signal design where the users share time and frequency simultaneously. Some studies [5], [7], [8] show that higher spectral efficiency can be achieved with NOMA techniques. The NOMA schemes are categorized as power domain multiplexing and code domain multiplexing including multiple access with low-density spreading (LDS), sparse code multiple access (SCMA), multiuser shared access (MUSA) and so on [9]. Some other proposed NOMA schemes are pattern division multiple access (PDMA), bit division multiplexing (BDM) and interleave division multiple access (IDMA). Software Defined Multiple Access (SoDeMA) has been proposed to address the issue of coexistence between different NOMA schemes. A simple classification of NOMA schemes is given as shown in Fig. 4-1 [10]. For NOMA, the users may be multiplexed and differentiated in the power domain, hence the name,

PD-NOMA. NOMA offers some significant capabilities that may assist in achieving the key performance metrics of diverse 5G use cases. Owing to the less complexity among all the schemes, the PD-NOMA has become the most studied scheme among all the NOMA schemes [5-7].

First, it utilizes the power domain multiplexing hence there is no need for orthogonality between user's shares either in time/frequency/code domain. Secondly, it can easily be implemented along with narrower beams for spatial multiplexing, providing a combination of power domain multiplexing and spatial multiplexing. This would be increasing the overall system capacity. Thirdly, SC and SIC are simple processes and have been well studied by the academia. Fourthly, as each of the user utilizes the complete resource block, it may transmit instantly as it requires, thereby reducing the overheads and increasing the latency. Last but not the least, other emerging techniques such as Multiple Input Multiple Output (MIMO) and millimeter waves (mmWaves) can also be combined with NOMA.

The foremost processes required in PD-NOMA are twofold. Superposition Coding of the user's signal at the transmitter, and subsequently Successive Interference Cancellation at the receiver side [10]. Both of the processes assist in achieving higher capacity of the system and are used jointly. The SC performs the vector superposition of the user's signal constellation, and SIC helps to increase the received SNR by the successive cancellation of the other user's signal (acting as interference).

## PRE-REQUISITES

*Channel Capacity:* The channel capacity for an Additive White Gaussian Noise (AWGN) channel for a point to point link, is represented in [11] as

$$C_{awgn} = W \log_2 \left( 1 + \frac{\bar{P}}{N_0 W} \right) \quad (1)$$

where,  $W$  is the channel bandwidth,  $\frac{\bar{P}}{N_0 W}$  is the signal-to-noise-ratio (SNR),  $\bar{P}$  is the power constraint in watts and  $N_0/2$  is the power spectral density (PSD) of Gaussian noise. *Spectral efficiency:* The spectral efficiency is a measure of the supported user data rate for a given bandwidth. Thus, the maximum bound for the spectral efficiency is determined by the channel capacity, which implies the maximum rate of information transfer per unit channel bandwidth

$$SE_{awgn} = W \log_2 (1 + SNR) \quad (2)$$

Equations (1) and (2) assume a discrete time baseband channel model described as  $y[m] = x[m] + w[m]$ , with  $x[m]$  as the input to the channel,  $y[m]$  being the channel output and  $w[m]$  is  $CN(0, N_0)$ . For a point-to-point link, the maximum user rate for a user  $i$ , can be represented as:

$$R_i = \log_2(1 + SNR_i) \quad (3)$$

where  $SNR_i$  is the SNR received at the  $i^{th}$  user, and  $SNR_i$  has an upper-bound suggested by (1) and (2). *Sum-rate*: The sum-rate, i.e. the sum of the rates of all the users in the network, is defined as

$$R_{sum} = \sum R_i \quad (4)$$

where,  $R_i$  is the  $i^{th}$  user throughput or data-rate [12].

Another performance indicator for 5G network, derived from the sum-rate is the energy efficiency (EE). EE is defined as the ratio of sum-rate with the total power consumed by the base station (BS) [13]. The sum-rate is also used to define the fairness index  $F$  for a network of  $K$  users as  $F = \frac{(\sum R_k)^2}{K \sum (R_k)^2}$  [13]. This fairness index represents a fair sharing of the system capacity between the users. The fairness index  $F=1$  implies all the users achieving the same capacity.

## THE SYSTEM MODEL

In pursuance of achieving the demands of 5G, the development of new architectures and configurations is the most essential task. Conducive to this, a profound analysis of the system model is required.

In this paper, we have analysed the system model of a simple NOMA network by considering a single antenna at the BS and two user-equipment (UE). In the downlink scenario, the BS is transmitting the superposed signal for both the users and the users have to decode their message from the superposed signal (Single Input Multiple Output, SIMO). For the uplink scenario, the BS receives the superposed signal of both the users, and the BS has to decode the user messages from the superposed signal (Multiple Input Single Output, MISO). In both the downlink and uplink, the users signal are weighted with different powers.

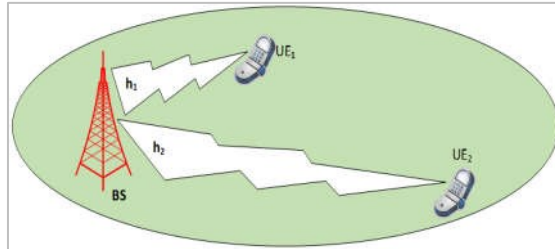


Figure 4-2 Single cell two-user NOMA downlink channel model

### A. DOWNLINK NOMA ANALYSIS

A single cell two user NOMA downlink channel model is shown in figure 4-2. For the downlink, the BS, depending upon the individual channel gains, performs this power allocation for the users. More power is allocated for the user with less channel gain (weaker user), and less power is allocated to the user with higher channel gain (stronger user). Further, we assume the channel gain to be constant over every transmission time Interval (TTI), i.e. the channel gain is quasi-static. In this case, first the weaker user decodes its signal from the superposed signal. The stronger user has to decode its own signal after cancelling the weaker user signal with the SIC process. As shown in the Fig.4-2, the NOMA cell consists of two users, at the cell-edge and around the centre of the cell. The BS forms the superposed signal to be transmitted to both of the users. This superposed signal is represented as:

$$x_s = P_1 x_1 + P_2 x_2 \quad (5)$$

where  $P_i$  is the allocated power for the symbol  $x_i$  of the  $i^{th}$  user. This superposed signal is to be received by the  $UE_1$  which has the point-to-point channel gain  $h$  between itself and the BS. The same superposed signal is also received by the  $UE_2$  which has the point-to-point channel gain  $h$  between itself and the BS. Without loss of generality, it is assumed that  $h_1 > h_2$  to designate the users as weaker user and stronger user. Now, the corresponding received signal  $y_1$  for  $UE_1$ , and  $y_2$  for  $UE_2$ , respectively are described as:

$$y_1 = h_1\sqrt{P_1}x_1 + h_1\sqrt{P_2}x_2 + n_1 \quad (6)$$

$$y_2 = h_2\sqrt{P_1}x_1 + h_2\sqrt{P_2}x_2 + n_2 \quad (7)$$

According to the NOMA principle,  $UE_2$  has to decode its message  $x_2$  considering  $x_1$  as an interference. The SNR for  $UE_2$  is then given as:

$$\gamma_2^{x_2} = \frac{|h_2|^2 P_2}{|h_2|^2 P_1 + 1} \quad (8)$$

where, the noise variance is assumed to be unity.

The  $UE_1$  performs SIC by cancelling the component with  $x_2$  from its received signal  $y_1$ . Hence, the SNR for  $UE_1$  becomes:

$$\gamma_1^{x_1} = |h_1|^2 P_1 \quad (9)$$

Based on (3) and using (8), (9), the rate  $R_i$  for  $UE_i$ ,  $i = 1, 2$  can be computed as follows.

$$R_1 = \log_2(1 + |h_1|^2 P_1) \quad (10a)$$

$$R_2 = \log_2\left(1 + \frac{|h_2|^2 P_2}{|h_2|^2 P_1 + 1}\right) \quad (10b)$$

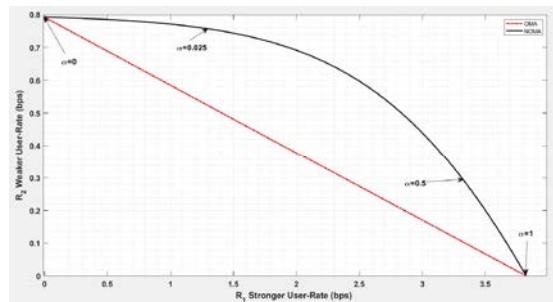


Figure 4-3 Capacity region plot for Downlink NOMA asymmetric channel

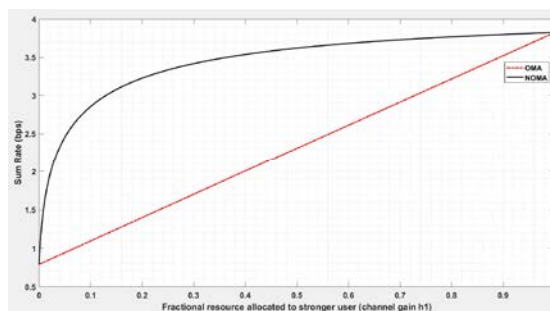


Figure 4-4 Sum-rate plot of Downlink NOMA asymmetric channel.

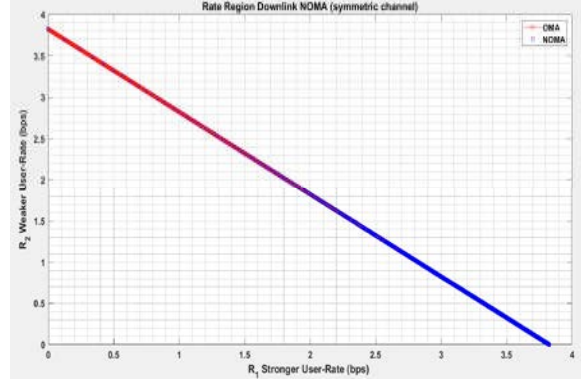


Figure 4-5 Rate region of Downlink NOMA symmetric channel.

From (8) and (9), it is clear that the user SNR increases as the allocated power to that user increases. For the downlink transmission, the BS allocates a limited power resource to the users, thereby, placing the power constraints as  $P_1, P_2 \geq 0$  and  $P_1 + P_2 = P$ , where  $P$  is the total power constraint of the BS. Considering the extreme cases, i.e. when the total power  $P$  is allocated to one of the users (say  $UE_1$ ) and no power is allocated to the other user, gives the maximum achievable rate or the capacity for that user (i.e.  $UE_1$ ). Now considering the power allocation factor, as the allocated power to the user performing SIC. Hence, the power of  $UE_1$  is given as  $P_1 = \alpha P$  and of  $UE_2$  is given as  $P_2 = (1 - \alpha)P = \bar{\alpha}P$ . We chose the power allocation factor to be the fractional power allocated to the stronger user and varied from 0 and 1, for the two extreme cases discussed above. Hence, by varying the parameter from 0 to 1, the set of rate points  $(R_1^*, R_2^*)$  are easily obtained as:

$$R_1^* = \log_2(1 + |h_1|^2 \alpha P) \quad (11a)$$

$$R_2^* = \log_2\left(1 + \frac{|h_2|^2 \bar{\alpha} P}{|h_2|^2 \alpha P + 1}\right) \quad (11b)$$

Varying  $\alpha$  from 0 and 1, we can obtain the two extreme cases discussed above.

For the improvement over 4G OFDMA (OMA) system, we consider the same scenario of two users, having weaker and stronger channels with the bandwidth allocation factor  $\tau$  that represents the fractional bandwidth allocated to the stronger user. Unlike the power allocation factor  $\alpha$ ,  $\tau$  is selected as 0.5, which implies equal bandwidth sharing between OMA users, to maintain user fairness. The capacity regions for Downlink NOMA as well as for Uplink NOMA were obtained for the downlink parameters given in [14]. The corresponding plot for the same parameters for downlink NOMA asymmetric channel is also obtained and is shown as Fig. 4-3. Moving further, the same capacity regions and sum-rate performance of Downlink NOMA for a symmetric channel are simulated and the plots are shown in fig. 4-4 for the sum-rate of asymmetric channel.

## B. UPLINK NOMA ANALYSIS

For the uplink, it is assumed that the  $UE$ 's transmit their signals with different power levels depending upon their distance from the BS and the channel conditions. More power is transmitted by the weaker user, and less power is transmitted by the stronger user. Just like the downlink case, we assume the channel is quasi-static. The simple uplink channel model for a single cell two user NOMA is shown in fig. 4-6. The uplink model is slightly different from the downlink NOMA model (5). In the uplink model, the BS receives the superposed signal of the users as:

$$x_{BS} = P_1 x_1 + P_2 x_2 + n_{BS} \quad (12)$$

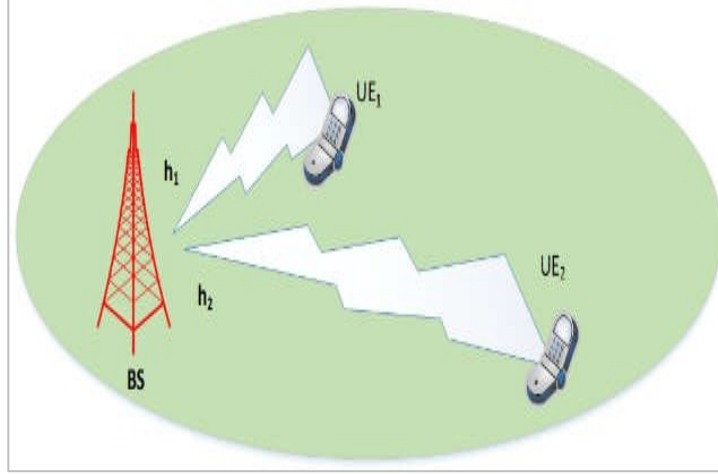


Figure 4-6 Single cell two-user NOMA uplink channel model

This superposed signal consists of  $UE_1$  signal  $x_1$  and  $UE_2$  signal  $x_2$ , and the AWGN noise is specified as  $n_{BS}$ .

Without the loss of generality, again we assume that  $h_1 > h_2$ , where  $h_i, i = 1, 2$  is the channel gain for  $UE_i$ , and  $n_{BS}$  is Gaussian noise with unity variance.

According to the NOMA principle, the BS has to decode one of the user signal first, treating the other user's signal as interference. Then the BS cancels the earlier decoded signal from the superposed signal (using SIC) to decode the other user's signal. Hence there are two possibilities, first is that the BS decodes  $UE_2$ , cancels  $UE_2$  signal from the superposed signal and then decodes  $UE_1$  signal. The second possibility is interchanging the user order, i.e. start with the decoding of  $UE_1$ , followed by cancellation of  $UE_1$  signal from the superposed signal and finally decoding  $UE_2$  signal.

According to the first possibility, the SNR for  $UE_2$  may be given as:

$$\gamma_2^{x_2} = \frac{|h_2|^2 P_2}{|h_1|^2 P_1 + 1} \quad (13)$$

where the noise variance is assumed unity. Following the SIC of  $UE_2$ , the SNR for  $UE_1$  then becomes:

$$\gamma_1^{x_1} = |h_1|^2 P_1 \quad (14)$$

Based on (3) and using (13), (14), the rate  $R_i$  for  $UE_i, i = 1, 2$  can be computed as following.

$$R_1 = \log_2(1 + |h_1|^2 P_1) \quad (15a)$$

$$R_2 = \log_2\left(1 + \frac{|h_2|^2 P_2}{|h_1|^2 P_1 + 1}\right) \quad (15b)$$

In the OMA case as seen earlier, the rate region is a straight-line segment joining the extreme points. We designate the point  $A(0, \log_2(1 + |h_2|^2 P_2))$  on the  $UE_2$  rate-axis and the point  $B(\log_2(1 + |h_1|^2 P_1), 0)$  on the  $UE_1$  rate-axis for this purpose.

Moreover, this straight line segment on the  $R_1 - R_2$  plane has a slope of  $\left(-\frac{\log_2(1 + |h_2|^2 P_2)}{\log_2(1 + |h_1|^2 P_1)}\right)$ .

It is interesting to observe from (15a) and (15b), if  $P_2 = 0$ , the point  $B$  becomes  $(0, 0)$  and point  $A$  attains a maximum  $A(0, \log_2(1 + |h_2|^2 P_2))$ . Also notice that if  $R_1 = 0$ , then the same points  $A$  and  $B$  are achieved and  $R_2 = \log_2(1 + |h_2|^2 P_2)$ . Similarly,  $P_1 = 0$  implies the point  $A$  becomes  $(0, 0)$  and point  $B$  attains a maximum  $(0, \log_2(1 + |h_1|^2 P_1))$ . Notice again, if  $R_2 = 0$ , then the same points  $A$  and  $B$  are achieved as  $R_1 = \log_2(1 + |h_1|^2 P_1)$ .

Hence, we conclude the order of SIC is important for the capacity analysis. Therefore, for the determination of capacity-region of NOMA, we consider both the decoding and SIC ordering possibilities.

First, we consider the case when the sequence of detection is- decoding of  $UE_2$  signal, followed by cancellation of  $UE_2$  signal from the superposed signal to decode  $UE_1$  signal. We consider a point as  $C$  on the  $R_1 - R_2$  capacity plane, having the coordinates of achievable rate-pair  $(R_1^*, R_2^*)$ . For the decoding and cancellation sequence considered above, the rate- pair is given as:

$$R_1^* = \log_2(1 + |h_1|^2 P_1) \quad (16)$$

$$R_2^* = \log_2\left(1 + \frac{|h_2|^2 P_2}{|h_1|^2 P_1 + 1}\right) \quad (17)$$

For the other decoding-cancellation sequence, we define another point  $D$  on the capacity plane, having the coordinates:

$$R_1^{**} = \log_2\left(1 + \frac{|h_1|^2 P_1}{|h_2|^2 P_2 + 1}\right) \quad (18)$$

$$R_2^{**} = \log_2(1 + |h_2|^2 P_2) \quad (19)$$

Finally, we have four set of points on the capacity plane, given as:

$$A(0, \log_2(1 + P_2 |h_2|^2)) \quad (20)$$

$$B(\log_2(1 + P_1 |h_1|^2), 0) \quad (21)$$

$$C(\log_2(1 + P_1 |h_1|^2), \log_2\left(1 + \frac{P_2 |h_2|^2}{P_1 |h_1|^2 + 1}\right)) \quad (22)$$

$$D(\log_2\left(1 + \frac{P_1 |h_1|^2}{P_2 |h_2|^2 + 1}\right), \log_2(1 + P_2 |h_2|^2)) \quad (23)$$

To determine the effect of power allocation on the capacity region that is defined by (20)-(23), we again employ a power allocation factor  $\alpha'$ , such that  $\alpha' = \frac{P_2}{P}$ .

The above capacity region points  $ABCD$  can then be expressed as:

$$A(0, \log_2(1 + \alpha' P |h_2|^2)) \quad (24)$$

$$B(\log_2(1 + (1 - \alpha') |h_1|^2), 0) \quad (25)$$

$$C(\log_2(1 + (1 - \alpha') |h_1|^2), \log_2\left(1 + \frac{\alpha' P |h_2|^2}{(1 - \alpha') |h_1|^2 + 1}\right)) \quad (26)$$

$$D(\log_2\left(1 + \frac{(1 - \alpha') |h_1|^2}{\alpha' P |h_2|^2 + 1}\right), \log_2(1 + \alpha' P |h_2|^2)) \quad (27)$$

Finally, plugging the values of various parameters from [14], and varying  $\alpha'$  from 0 to 1, the characteristics of the capacity region may be deduced. Fig. 4-7 shows the obtained capacity region for a symmetric channel. As seen from fig. 4-7, we observe that the maximum permissible user throughput achieved in NOMA uplink in a symmetric channel is less than the maximum permissible user-throughput achieved in OMA.

Figure 4-8 shows the variation of the points  $ABCD$ , and from here the symmetric capacity can be derived. This symmetric capacity is the common maximum rate at which the user's can transmit. In fig. 4-8, this symmetric capacity is given by the intersection of the locus of points  $C$  and  $D$ .

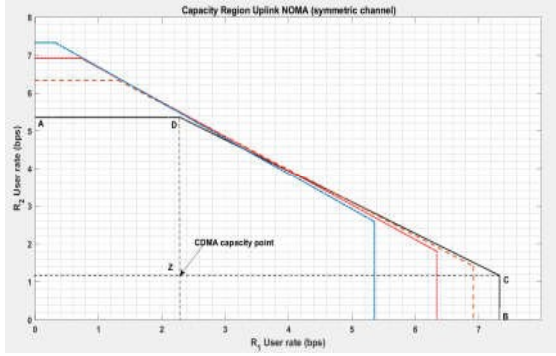


Figure 4-7 Capacity region for Uplink NOMA for symmetric channel ( $|h_1| = |h_2|$ )

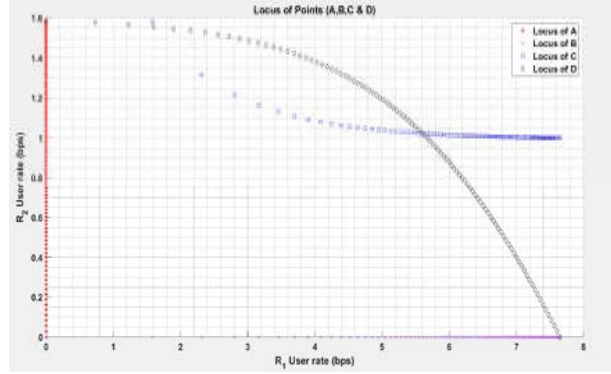


Figure 4-8 Variation of capacity-region points with power allocation factor

## SIMULATION AND INTERPRETATION

The simulation for the analysis was carried out in MATLAB 9.6.0.1214997 (R2019a) Update 6 on a windows operating system with Intel i-5 dual core processor@ 2.9 GHz and 8GB installed RAM. For the simulation of the two user NOMA cell (downlink), the channel gain for user ( $h_1$ ) and for user ( $h_2$ ) were selected to be  $h_1 = \sqrt{5}$  and  $h_2 = \sqrt{5}/10$ , for asymmetric channel, and the power constraint = 40 . These values were taken from [14]. The obtained results can be grouped into two categories- asymmetric channel, and symmetric channel.

### A. ASYMMETRIC CHANNEL

For the asymmetric channel, we assumed unequal channel gains  $h_1$  and  $h_2$ . The user-rate obtained for the downlink case are shown in fig. 4-3, with the solid-red line representing the achievable user-rate for the two user OMA network, and the solid-black line representing the NOMA network. Both the curves meet at the power allocation factor values of 0 and 1 that shows the single-user maximum rate is the same for both OMA and NOMA network. However, between these two extreme values (0 and 1), the NOMA network shows significant rate-increase. As user  $UE_1$  is stronger user, therefore the SIC has to be done by  $UE_1$ , and  $UE_2$  simply decodes its own data without SIC. As we can see from fig. 4-3, allocation of more power to the stronger user reduces the user-rate of weaker user. This happens when the power allocation factor is increased towards one. Further, fig. 4-3 also shows the achievable rate when OMA is used. We considered equal bandwidth and equal power allocated to both the users in OMA so as to maintain the fairness in the system. The comparison of the curves indicate the superiority of NOMA over OMA in downlink scenario with different channel gains. Now, if large power is allocated to the stronger user, then the weaker user rate approaches zero. Hence, in this scenario, the weaker user should be allocated higher power.

Fig. 4-4 shows the variation of sum-rate with the power allocation factor, which again confirms that both the networks have the same sum-rate at the extreme values of power allocation factor.

However, allocating a large power to the stronger user does not vary the sum-rate significantly, whereas allocating less power to the stronger user varies the sum-rate significantly, that can be observed by the larger slope of the NOMA curve in fig. 4-4.

### B. SYMMETRIC CHANNEL

For the symmetric channel, we assume equal channel gains  $h_1$  and  $h_2$ . The user-rates obtained for the downlink case are shown in fig. 4-5, with the solid-red line representing the achievable user-rate for the two user OMA network, and the solid-blue line representing the NOMA network. This suggests that under the same channel conditions, both the networks have same rate-regions, thus have a similar performance. Hence, the

performance is NOMA is not inferior to OMA even under symmetric channel case. For the uplink scenario the same channel gains were assumed as for the downlink, and the results are plotted in Fig. 4-7 and Fig. 4-8.

For the symmetric channel, it was observed that the optimum rate region points i.e. points *C* and *D* require a specific range of power allocation factor to maintain the given quality of service to the users.

Hence based on these curves, an optimum range of power allocation factor could be decided for required guaranteed quality of service to the users. Further, even for the symmetric channel conditions, the rates offered are much higher than the CDMA scheme. Finally, fig. 4-8 shows the variation of the points ABCD of the capacity region with the power allocation factor. The loci of these points would help in the visualization of the capacity region for the symmetric case.

## CONCLUSION

The basic models for uplink and downlink NOMA systems are analyzed in depth, and the simulated results are in agreement with the theoretical NOMA models presented in earlier literatures. A number of observations can be made related to our work. First, it justifies the superiority of NOMA over the existing multiple access techniques. Properly chosen power allocation ratio, both in the uplink and in the downlink could significantly increase the user-throughput than compared to the OMA schemes. Another result obtained is that even under the same channel conditions the performance of NOMA is not inferior to OMA. The results may help to suggest the optimum achievable rate region for a given power allocation coefficient. Thus, determining this optimum region will be an imperative aspect for the researchers. We analyzed the system for two users, but we expect that to utilize NOMA, more users can be accommodated to the network. This would be our future work.

## ACKNOWLEDGEMENT

We thank Dr. S.S. Sahu, Prof. S. Pal and Prof. Nisha Gupta, from ECE Department, BIT Mesra, for providing valuable suggestions and resources to carry out this work.

## REFERENCES

- [1] "Internet of Things forecast," Ericsson, 2019. [Online]. Available: <https://www.ericsson.com/en/mobilityreport/internet-of-things-forecast>
- [2] Rachid El Hattachi; Javan Erfanian, "NGMN 5G White Paper," NGMN, 2015.
- [3] D. Tse and P. Viswanath, *Fundamentals of Wireless Communications*, Cambridge University Press, 2005.
- [4] S. Kumar, *Wireless Communication: The Fundamental & Advanced Concepts*, River Publishers, Denmark , 2015.
- [5] R. C. Kizilirmak, "Non-Orthogonal Multiple Access (NOMA) for 5G Networks," in *Towards 5G Wireless Networks : A physical layer perspective*, Intech Open, 2016, pp. 83-98.
- [6] E. Mohyeldin, "Minimum Technical Performance Requirements for IMT-2020 Radio Interface(s)," NOKIA, 2017.
- [7] C. Xiong, G. Li, S. Zhang, Y. Chen and S. Xu, "Energy and Spectral Efficiency Tradeoff in Downlink OFDMA networks," *IEEE Transactions on Wireless Communications*, vol. 10, no. 11, pp. 3874-3886, 2011.
- [8] M. Aldababsa, M. Toka, S. Gokceli, G. K. Kurt and O. Kucur, "A tutorial on Nonorthogonal Multiple Access for 5G and Beyond," *Wireless Communications and Mobile Computing* , vol. 2018, pp. 1-24, 2018.
- [9] M. Vaezi, Z. Ding and H. V. Poor, Eds., *Multiple Access Techniques for 5G Wireless Networks and Beyond*, Springer, 2019.
- [10] K. HUGUCHI and Anas BENJEBBOUR, "Nonorthogonal Multiple Access (NOMA) with Successive Interference Cancellation for Future Radio Access," *IEICE Transactions on Communication*, Vols. E-98, no. 3, 2015.
- [11] Q. C. Li, H. Niu, A. Papatnassiou and G. Wu, "5G network capacity: Key elements and technologies," *IEEE Vehicular Technology*, vol. 9, no. 1, pp. 71-78, 2014.
- [12] L. Dai, B. Wang, Y. Yuan, S. Han, C.-L. I and Z. Wang, "Non-orthogonal multiple access for 5G: solutions, challenges, opportunities, and future research trends," *IEEE Communications*, vol. 53, no. 9, pp. 74-81, 2015.
- [13] S. M. R. Islam, N. Avazov, O. A. Dobre and K.-S. Kwak, "Power-Domain Non-Orthogonal Multiple Access (NOMA) in 5G Systems: Potentials and Challenges," *IEEE Communication Surveys and Tutorials*, vol. 19, no. 2, pp. 721-741, 2017.
- [14] M. Vaezi, R. Schober, Z. Ding and H. Poor, "Nonorthogonal Multiple Access: Common Myths and Critical Questions," *IEEE Wireless Communications* , vol. 26, no. 5, pp. 174-180, 2019.
- [15] A. Benjebbour, Y. Saito, Y. Kishiyama, A. Li, A. Harada and T. Nakamura, "Concept and Practical considerations of Non-orthogonal Multiple Access (NOMA) for Future Radio Access," in *2013 International Symposium on Intelligent Signal Processing and Communication Systems*, Naha, Japan, 2013.
- [16] L. Dai, B. Wang, Z. Ding, Z. Wang, S. Chen and L. Hanzo, "A survey of Non-orthogonal Multiple Access for 5G," *IEEE Communications Surveys and Tutorials*, vol. 20, no. 3, pp. 2294-2323, 2018.

- [17] K. Yang, N. Yang, N. Ye, M. Jia, Z. Gao and R. Fan, "Non-orthogonal Multiple Access: Achieving Sustainable Future Radio Access," *IEEE Communications Magazine*, vol. 57, no. 2, pp. 116-121, 2019.
- [18] Q. C. Li, H. Niu, A. Papathanassiou and G. Wu, "5G network capacity: Key elements and technologies," *IEEE Vehicular Technology*, vol. 9, no. 1, pp. 71-78, 2014.
- [19] L. Dai, B. Wang, Y. Yuan, S. Han, C.-L. I and Z. Wang, "Non-orthogonal multiple access for 5G: solutions, challenges, opportunities, and future research trends," *IEEE Communications*,